


Calciprotein particle inhibition explains magnesium-mediated protection against vascular calcification

Anique D. ter Braake¹, Coby Eelderink², Lara W. Zeper¹, Andreas Pasch^{3,4}, Stephan J.L. Bakker², Martin H. de Borst², Joost G.J. Hoenderop¹ ¹ and Jeroen H.F. de Baaij¹ ¹

¹Department of Physiology, Radboud Institute for Molecular Life Sciences, Radboud University Medical Center, Nijmegen, The Netherlands, ²Division of Nephrology, Department of Internal Medicine, University Medical Center Groningen, Groningen, The Netherlands, ³Calciscon AG, Nidau, Switzerland and ⁴Institute for Physiology and Pathophysiology, Johannes Kepler University Linz, Linz, Austria

Correspondence to: Jeroen H.F. de Baaij; E-mail: jeroen.debaaij@radboudumc.nl

ABSTRACT

Background. Phosphate (Pi) toxicity is a strong determinant of vascular calcification development in chronic kidney disease (CKD). Magnesium (Mg^{2+}) may improve cardiovascular risk via vascular calcification. The mechanism by which Mg^{2+} counteracts vascular calcification remains incompletely described. Here we investigated the effects of Mg^{2+} on Pi and secondary crystalline calciprotein particles (CPP2)-induced calcification and crystal maturation.

Methods. Vascular smooth muscle cells (VSMCs) were treated with high Pi or CPP2 and supplemented with Mg^{2+} to study cellular calcification. The effect of Mg^{2+} on CPP maturation, morphology and composition was studied by medium absorbance, electron microscopy and energy dispersive spectroscopy. To translate our findings to CKD patients, the effects of Mg^{2+} on calcification propensity (T_{50}) were measured in sera from CKD patients and healthy controls.

Results. Mg^{2+} supplementation prevented Pi-induced calcification in VSMCs. Mg^{2+} dose-dependently delayed the maturation of primary CPP1 to CPP2 *in vitro*. Mg^{2+} did not prevent calcification and associated gene and protein expression when added to already formed CPP2. Confirmatory experiments in human serum demonstrated that the addition of 0.2 mmol/L Mg^{2+} increased T_{50} from healthy controls by 51 ± 15 min ($P < 0.05$) and CKD patients by 44 ± 13 min ($P < 0.05$). Each further 0.2 mmol/L addition of Mg^{2+} led to further increases in both groups.

Conclusions. Our results demonstrate that crystalline CPP2 mediates Pi-induced calcification in VSMCs. *In vitro*, Mg^{2+} delays crystalline CPP2 formation and thereby prevents Pi-induced calcification.

Keywords: calciprotein particle, calcification propensity, chronic kidney disease, magnesium, vascular calcification

INTRODUCTION

Vascular calcification contributes to cardiovascular morbidity and mortality in chronic kidney disease (CKD) [1]. Currently treatment options are limited and persisting vascular calcification remains a clinical problem. In past years, several epidemiological studies have shown that a lower serum magnesium (Mg^{2+}) status is independently associated with an increased risk of vascular calcification and cardiovascular mortality in CKD patients [2–4]. Therefore it is hypothesized that Mg^{2+} could be an effective tool to limit vascular calcification [5]. However, the mechanisms underlying the potent anti-calcification properties of Mg^{2+} are incompletely understood.

Hydroxyapatite- and protein-containing calciprotein particles (CPPs) are major drivers of calcification [6, 7]. The transition from calcium (Ca^{2+})- and phosphate (Pi)-containing amorphous or primary CPP1 towards crystalline or secondary CPP2 is key in the development of vascular smooth muscle cell (VSMC) calcification [6, 8]. Due to disturbances in the bone-mineral axis, resulting from elevated Pi and decreased calcification inhibitors such as matrix gla protein (MGP) and fetuin-A, high Pi levels crystallize into CPP2 [7, 9]. These events result in active reprogramming of VSMCs, which in turn enhances the calcification process by up-regulating osteogenic genes, producing excess extracellular matrix, undergoing apoptosis and releasing pro-calcific exosomes [10–12].

Since VSMCs may activate osteogenic pathways that contribute to calcification, the capacity of Mg^{2+} to inhibit vascular calcification may rely on direct modulation of these cellular processes [13]. Indeed, multiple studies demonstrate that Mg^{2+} did not inhibit calcification upon transient receptor potential melastatin 7 blocking, an abundant Mg^{2+} channel in VSMCs, implying that intracellular Mg^{2+} prevents calcification [14, 15]. In addition, Mg^{2+} supplementation *in vitro* correlates with

reduced expression of pro-calcification genes and with increased expression of calcification protectors [16–18]. On the contrary, in the extracellular compartment, Mg^{2+} has potent anti-crystallization properties, which have been shown to be of importance in its capacity to prevent VSMC calcification *in vitro* [19–22].

The importance of CPP2 in the development of vascular calcification has been exploited in a novel diagnostic tool where the intrinsic capacity of patient serum to prevent the transition from CPP1 to CPP2, or calcification propensity of the serum, can be measured using the T_{50} test [7, 23, 24]. The identification of factors affecting T_{50} is of interest in the context of clinical management of vascular calcification, as these factors may influence the development and progression of vascular calcification in renal disease patients [23, 25–27]. T_{50} is correlated with cardiovascular mortality and is affected by Pi [23]. Therefore, whether Pi toxicity resulting in increased risk for vascular calcification is determined by the presence of soluble Pi or that Pi toxicity is mediated by crystallization in CPP2 is important to consider.

In this study we aimed to delineate the mechanisms that explain the effects of Mg^{2+} on VSMC calcification. In our study we induced VSMC calcification using both Pi and CPP2, which allows comparison of the direct and indirect effects of Mg^{2+} supplementation on VSMC calcification. Using scanning electron microscopy (SEM) and energy dispersive spectroscopy (EDX), we studied CPP transition, morphology and composition in the presence and absence of Mg^{2+} *in vitro*. Furthermore, we studied the influence of Mg^{2+} on calcification propensity in serum from CKD patients and healthy controls *ex vivo*.

MATERIALS AND METHODS

Cell culture

Human aortic VSMCs (hVSMCs) were purchased from the American Type Culture Collection (Manassas, VA, USA, lot no. PCS-100-012) and cultured in Dulbecco's Modified Eagle Medium (DMEM; Lonza, Basel, Switzerland) consisting of 20% (v/v) foetal bovine serum (FBS; BioWest, GE Healthcare, Little Chalfont, UK), 2 mmol/L L-glutamine and 10 μ g/mL ciprofloxacin at 37°C in a humidified incubator containing 5% carbon dioxide (CO_2 ; v/v). Cells were used until the 10th passage. For calcification experiments, cells were cultured in 12-well plates and switched to calcification medium at subconfluence. Calcification medium consisted of 5% FBS (v/v) and 3 mmol/L Pi (NaH_2PO_4), and 2 mmol/L Mg^{2+} when indicated. Cells were cultured for up to 8 days. The medium was changed every 2–3 days.

CPP synthesis, isolation and induction of calcification

Phenol red-free DMEM (Gibco, Thermo Fisher Scientific, Waltham, MA, USA) was supplemented with 3.5 mmol/L NaH_2PO_4 , 1 mmol/L calcium chloride, 10% FBS (v/v), 2 mmol/L L-glutamine and 10 μ g/mL ciprofloxacin and stored in a humidified incubator at 37°C containing 5% CO_2 (v/v) for 14 days. For isolation of CPP2, CPP-containing media were centrifuged at 16 000 g for 30 min at room temperature. The

pellet was resuspended in DMEM containing 10 μ g/mL ciprofloxacin and stored at 4°C. The Ca^{2+} content of the CPP2 suspension was measured using the *o*-cresolphthalein complexone method as described elsewhere [19]. Cells were treated with CPP2 at a final concentration ranging from 5 to 100 μ g/mL Ca^{2+} (5–100 CPP). Cells were cultured in their designated media for up to 4 days without a change of media.

Analysis of VSMC calcification

Quantification of total cellular Ca^{2+} deposition using the *o*-cresolphthalein complexone method and alizarin red staining were performed as previously described [19].

Gene expression analysis

Total RNA was isolated from hVSMCs using TRIzol (Invitrogen, Thermo Fisher Scientific) according to the manufacturer's instructions. Genomic DNA was removed by DNase treatment prior to complementary DNA synthesis from 1 μ g total RNA (Promega, Madison, WI, USA). The primers used for polymerase chain reaction (PCR) amplification were equally efficient (Supplementary data, Table S1). Reverse transcription quantitative PCR was executed in duplicate using IQ SYBRGreen Mix (Bio-Rad, Hercules, CA, USA) according to the manufacturer's protocol in a Bio-Rad thermocycler. The expression levels of genes of interest were normalized to *GAPDH* expression levels.

Protein expression analysis

To prepare total lysate of hVSMCs, the hVSMC monolayer was scraped in a 1% (v/v) Triton-X100 lysis buffer containing protease inhibitors. The protein concentration was determined using the Pierce BCA Kit according to the manufacturer's instructions (Thermo Fisher Scientific Waltham). Subsequently samples consisting of equal amounts of protein were denatured in Laemmli buffer containing 10 mmol/L dithiothreitol and applied to sodium dodecyl sulphate–polyacrylamide gel electrophoresis. Blots were incubated at 4°C overnight with primary antibodies against osteopontin (OPN; 1:1000; R&D Systems, Minneapolis, MN, USA; #MAB14331-100), transgelin (SM22 α ; 1:5000; Abcam, Cambridge, UK; #ab14106) and MGP (1:500; Proteintech, Rosemont, IL; #10734-1-AP). Blots were subsequently incubated with horseradish peroxidase conjugated secondary antibodies for 1 h at room temperature. Band intensity was measured using ImageJ software (National Institutes of Health, Bethesda, MD, USA) and expression was corrected for β -actin and expression levels per group were normalized to the control.

Electron microscopy

CPPs were transferred onto copper tape, coated with carbon and used for SEM analysis (GeminiSEM, Zeiss, Oberkochen, Germany) and EDX for elemental analysis (QUANTAX 200, Bruker, Billerica, MA, USA). Images were obtained using an Everhart–Thornley secondary electron detector (Bruker) at 5 kV for morphological observations and 20 kV for microelemental analyses. For transmission EM (TEM), the CPP solution was transferred onto a Formvar-coated copper grid and air

dried. TEM was performed on a JEOL JEM 1400 microscope (JEOL USA, Peabody, MA, USA) with an accelerating voltage of 60 kV. Images were acquired at 15 000-fold magnification (Gatan, Pleasanton, CA, USA).

CPP maturation assay

CPP2 were generated in phenol red-free DMEM (Gibco) containing 10% FBS and MgCl_2 was added to reach 1.0, 1.2, 1.4, 1.6, 1.8 and 2.0 mmol/L. As a reference, medium containing 10% FBS (v/v) was included. CPP2 maturation was monitored by daily measurement of the absorption at 570 nm for 14 days using a Benchmark Plus Microplate Spectrophotometer System (Bio-Rad) [6]. A separate group where MgCl_2 was added only after absorption exceeded 0.15 (after 5 days) was included to study the effects of Mg^{2+} on already formed CPP2 and monitored until complete ripening after 14 days. To study the effects of high Pi on the inhibition of CPP2 by 2.0 mmol/L Mg^{2+} , CPP2 maturation was monitored in the presence of 4 and 5 mmol/L Pi (final concentration) in addition to the standard CPP mixture in a separate experiment. To test a potential role for Mg^{2+} in altering the pH of the CPP mixtures, pH was measured for the CPP mixtures without Mg^{2+} and with 2.0 mmol/L Mg^{2+} at 0, 7 and 14 days of incubation.

Calcification propensity (T_{50} test) in serum samples supplemented with Mg^{2+}

Serum samples collected prior to transplantation from renal transplant recipients (CKD patients) and donors (healthy controls) of the TransplantLines cohort study (METc UMCG No. 2014/077, NTC03272841) were used in this study [28]. Blood from 10 subjects per group was collected in 4 mL serum collection tubes and centrifuged at 1300 g for 10 min at room temperature. Serum was stored at -80°C until analysis. The T_{50} test (calcification propensity) has been described previously [24]. Serum was subjected to the T_{50} test without any additions (baseline) and after addition of solutions with MgCl_2 resulting in increased concentrations of 0.2, 0.4, 0.6, 0.8 and 1.0 mmol/L. After 570 min, the test was terminated. Other laboratory measurements were performed during routine clinical visits prior to serum collection for this study (Supplementary data, Table S2).

Statistical analysis

Parametric data were analysed by one-way analysis of variance (ANOVA) with Tukey's *post hoc* test to correct for multiple comparisons using PRISM software (GraphPad Software, San Diego, CA, USA). Non-parametric data as identified by the Shapiro–Wilk test for normality were analysed using Kruskal–Wallis analysis with Dunn's correction for multiple comparisons. For grouped analysis, data were analysed using a two-way ANOVA. All data are shown as mean \pm standard deviation (SD). P-values <0.05 were considered statistically significant.

RESULTS

Mg^{2+} prevents high Pi-induced VSMC calcification

To study the preventive effect of Mg^{2+} on *in vitro* calcification, VSMCs were cultured in Pi medium and supplemented

with MgCl_2 (Figure 1). VSMCs cultured in high Pi showed calcification, as visualized by the alizarin red staining (Figure 1A) and as quantified by the *o*-cresolphthalein complexone method for Ca^{2+} (Figure 1B). VSMCs cultured in high Pi supplemented with Mg^{2+} stained negative for alizarin red and Ca^{2+} deposition was reduced by >100 -fold versus high Pi-treated VSMCs after 8 days (28 ± 12 versus $2990 \pm 1800 \mu\text{g Ca}^{2+}/\text{mg protein}$; $P < 0.05$). The preventive effect of Mg^{2+} on hVSMC calcification was preserved at 4 and 5 mmol/L Pi (Supplementary data, Figure S1). To evaluate the effect of Mg^{2+} on genetic changes induced by calcification in VSMCs, the gene expression of calcification inducers alkaline phosphatase (*ALP*) and *OPN* and calcification inhibitor *MGP* in addition to contractile markers calponin (*CNN1*) and *SM22 α* were studied (Figure 1C). Compared with control VSMCs, VSMCs cultured in 3 mmol/L Pi had a 40–60% reduction in *ALP* and *SM22 α* gene expression after both 6 and 8 days of incubation ($P < 0.05$). *MGP* mRNA expression remained stable. After high Pi treatment for 8 days, VSMCs expressed only $\sim 20\%$ of *CNN1* gene expression compared with control VSMCs ($P < 0.05$). Pi-treated VSMCs did not change *OPN* gene expression. Mg^{2+} supplementation in addition to high Pi preserved the levels of *MGP*, *ALP*, *SM22 α* and *CNN1* gene expression versus control VSMCs. VSMCs treated with 2 mmol/L Mg^{2+} alone and in combination with 3 mmol/L Pi showed a non-significant downregulation of *OPN* after 8 days. On a protein level, *OPN* was increased 2-fold by Pi treatment ($P < 0.05$). Furthermore, *SM22 α* protein expression was decreased after 8 days of Pi treatment. In high Pi-treated hVSMCs supplemented with Mg^{2+} , both the increased *OPN* and decreased *SM22 α* protein expression were normalized. *MGP* protein expression remained stable in all treatment groups (Figure 1D).

CPPs induce VSMC calcification independent of Mg^{2+}

To be able to distinguish between intracellular and extracellular actions of Mg^{2+} , the effects of Mg^{2+} on CPP2-induced VSMC calcification were assessed (Figure 2). Alizarin red staining (Figure 2A) and Ca^{2+} deposition measurements (Figure 2B) showed increased calcification after 24 h in VSMCs treated with 50 CPP2 (488 ± 62 versus $2 \pm 2 \mu\text{g Ca}^{2+}/\text{mg protein}$; $P < 0.05$). Mg^{2+} supplementation to CPP2-treated VSMCs did not reduce Ca^{2+} deposition compared with CPP2-only treated VSMCs after 24 h (488 ± 62 versus $565 \pm 62 \mu\text{g Ca}^{2+}/\text{mg protein}$) and 4 days (657 ± 132 versus $783 \pm 142 \mu\text{g Ca}^{2+}/\text{mg protein}$, respectively). CPP2 treatment decreased *CNN1* gene expression by almost 50% after both 2 days and 4 days (Figure 2C; $P < 0.05$). CPP2 treatment resulted in downregulation of *OPN* and *ALP* after 2 days, which seemed to be prevented by Mg^{2+} . *SM22 α* mRNA expression was decreased after 2 days of CPP treatment and after 4 days of Mg^{2+} -supplemented CPP2 treatment. Protein concentrations of *OPN* were increased ~ 4 -fold in both CPP2-treated hVSMCs with and without 2 mmol/L Mg^{2+} (Figure 2D). *SM22 α* protein expression showed a non-significant trend towards a reduction in CPP2-treated cells independent of Mg^{2+} . *MGP* protein expression was stable in all treatment groups. To test whether Mg^{2+} might prevent CPP-induced calcification at lower CPP2

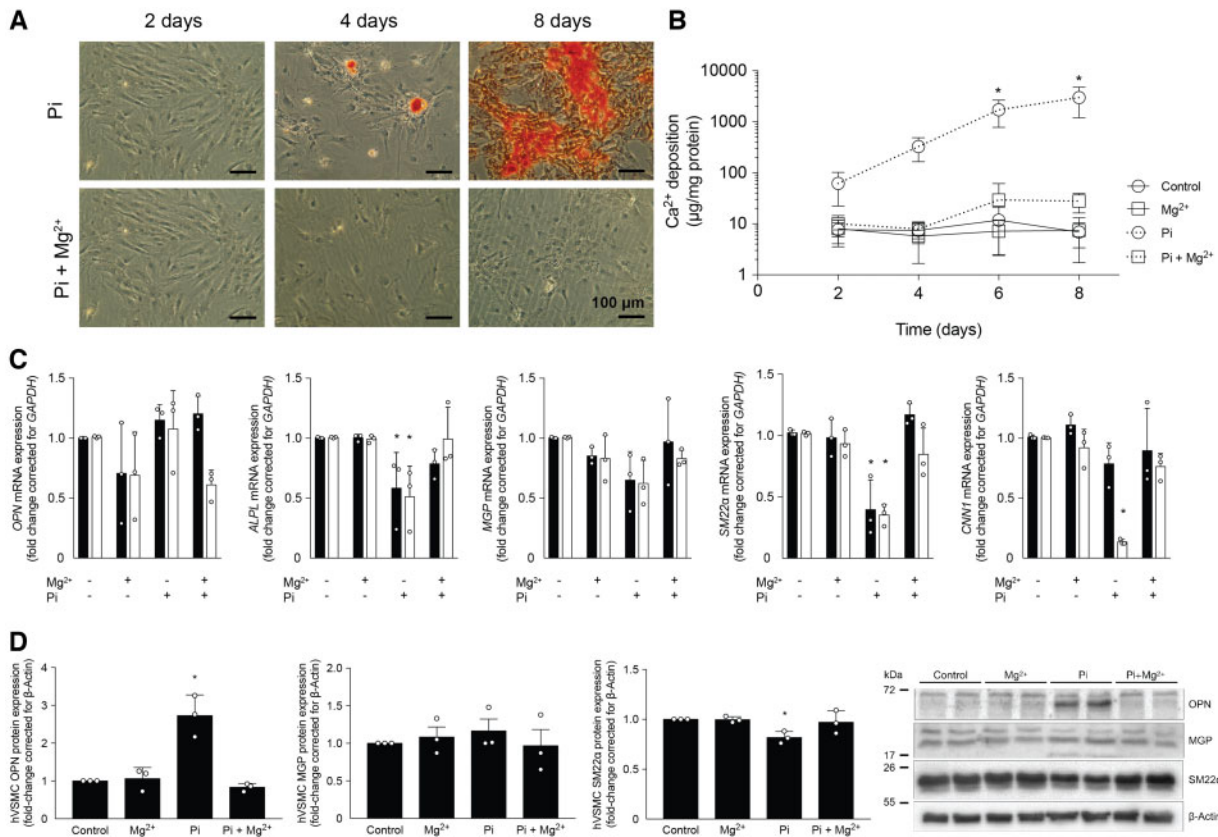


FIGURE 1: Mg^{2+} prevents Pi-induced calcification in hVSMCs. (A) Alizarin red staining was negative in Mg^{2+} -supplemented Pi cultures, indicating the absence of calcification after 2, 4 and 8 days. (B) Ca^{2+} deposition on VSMCs was increased in Pi-treated cells compared with controls, but was absent after 2.0 mmol/L Mg^{2+} supplementation. (C) Pi-induced calcification decreased ALP and non-significantly decreased calcification inhibitor *MGP* and VSMC contractile genes *SM22 α* and *CNN1* after 6 days (black bars) and 8 days (white bars) of incubation, which was prevented by Mg^{2+} . (D) Protein expression of OPN, *SM22 α* and *MGP* was measured and quantified. Data are shown as fold changes compared with the day-matched controls and presented as the mean of three separate experiments, consisting of three replicate cultures \pm SD. * $P < 0.05$ versus day-matched control.

concentrations, Mg^{2+} was supplemented to VSMCs treated with a broad range of CPP2 dosages (Figure 3). Both 2 and 5 mmol/L Mg^{2+} did not reduce VSMC Ca^{2+} deposition at any of the CPP2 dosages, ranging from 5 to 100 CPP. Compared with CPP2 treatment containing no additional Mg^{2+} , supplementation of 5 mmol/L Mg^{2+} resulted in increased Ca^{2+} deposition at 25, 50 and 75 CPP2 [$82 \pm 5\%$ versus $99 \pm 16\%$ at 75 CPP ($P < 0.05$), respectively, where 100 CPP2 with no additional Mg^{2+} is set to 100% calcification].

Mg^{2+} dose-dependently prevents secondary CPP maturation

To study the action of Mg^{2+} on CPP transition *in vitro*, CPP medium was incubated to form CPP1 and CPP2 in the presence of a range of $MgCl_2$ concentrations. CPP medium showed an initial increase in absorbance reflecting CPP1 formation after 1 day (absorbance change from 0.042 to 0.055) and the second increase in absorbance reflecting CPP2 formation after 3 days (absorbance change from 0.055 to 0.138; Figure 4A). Mg^{2+} supplementation resulted in a similar increase in absorbance after 1 day of culture (absorbance change of supernatant from 0.042 to 0.057 for 2.0 mmol/L Mg^{2+}). Mg^{2+} final concentrations of 1.6,

1.8 and 2.0 mmol/L preserved the CPP1 state for 14 days (final absorbance 0.077). A final concentration of 1.0, 1.2 and 1.4 mmol/L delayed the second increase in absorbance by 1, 7 and 11 days, respectively. In the presence of 4 and 5 mmol/L Pi, 2 mmol/L Mg^{2+} inhibited CPP1 to CPP2 transition (Supplementary data, Figure S1). Increasing Mg^{2+} to a concentration of 2.0 mmol/L to CPP medium after CPP2 had formed (on Day 5) did not result in changes in the absorption of the CPP medium (final absorbance 0.170 versus 0.174). After 14 days, CPP2 and CPP2 supplemented with Mg^{2+} were isolated and analysed by EM and EDX to study CPP characteristics (Figure 4B–G). Mg^{2+} supplementation did not affect the pH of the CPP mixture (Supplementary data, Figure S2). SEM revealed similar morphology of the CPP2 independent of Mg^{2+} treatment (Figure 4B and E). EDX peaks were present at energy levels corresponding to enriched Pi and Ca^{2+} (Figure 4C and F). Quantification of the peaks showed that Mg^{2+} -supplemented CPP2 contains 37.1% oxygen, 18.7% Pi and 39.4% Ca^{2+} , which did not significantly differ from CPP2 without Mg^{2+} supplementation (Figure 4D and G). In addition, there was a slight trend towards increased Na^+ , Cl^- and Mg^{2+} content in Mg^{2+} -supplemented CPP2, but this was not statistically significant.

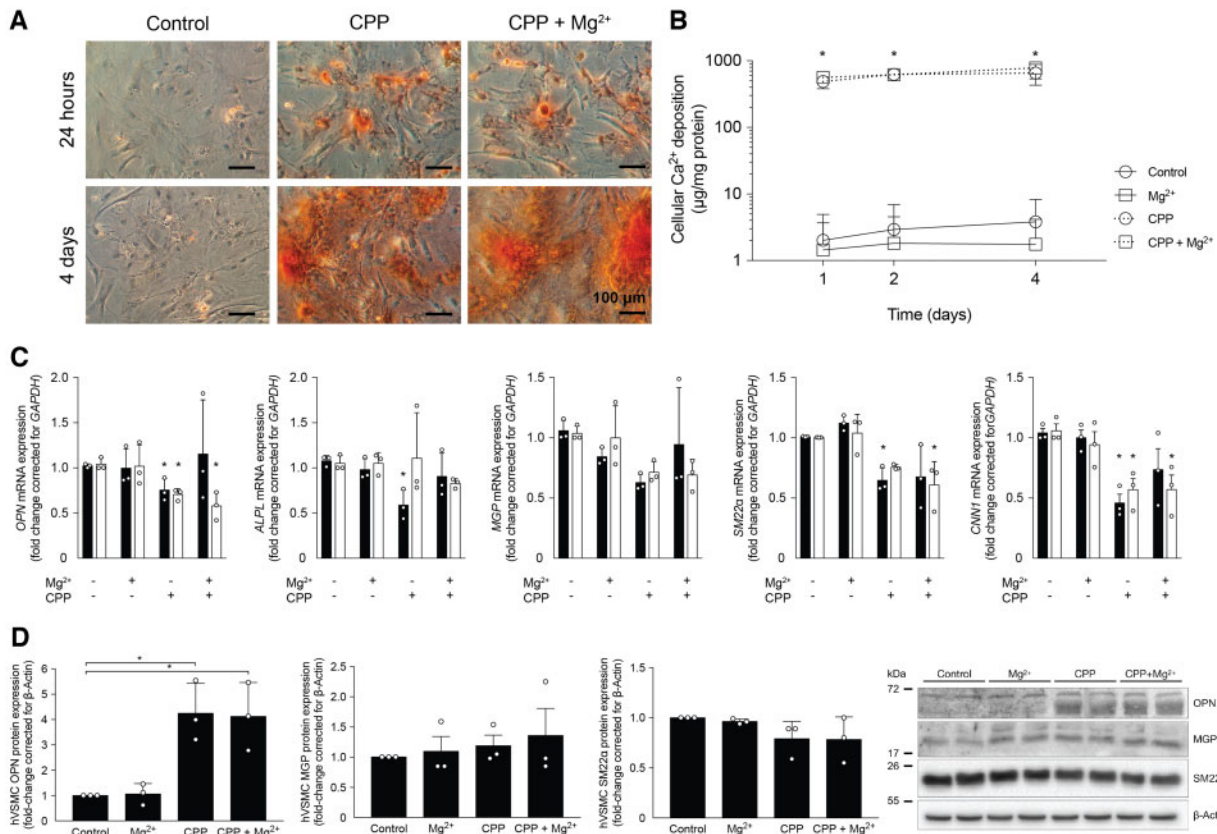


FIGURE 2: Mg^{2+} does not prevent CPP2-induced calcification in hVSMCs. (A) Alizarin red staining and (B) Ca^{2+} deposition quantification show that CPP2-induced calcification is not prevented by 2.0 mmol/L Mg^{2+} after 24 h and 4 days. (C) Gene expression related to calcification after CPP2 treatment was measured after 2 days (black bars) and 4 days (white bars) and remained unchanged by Mg^{2+} . (D) Protein expression of OPN, SM22 α and MGP was measured and quantified. Data are shown as fold changes compared with the day-matched controls and presented as the mean of three separate experiments, consisting of three replicate cultures \pm SD. * $P < 0.05$.

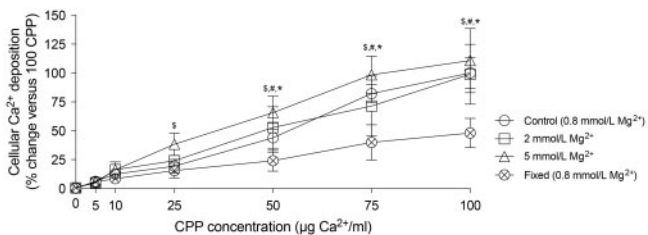


FIGURE 3: High Mg^{2+} concentration stimulates CPP2-induced calcification. Ca^{2+} deposition was measured after incubation of VSMCs for 24 h with varying CPP2 concentrations in the presence of 0.8 (control), 2 and 5 mmol/L Mg^{2+} . Mg^{2+} did not prevent CPP2-induced calcification at any CPP concentration. At 5 mmol/L, Mg^{2+} increased cellular Ca^{2+} deposition at CPP2 concentrations of 25, 50 and 75 μ g/mL Ca^{2+} versus CPP2 treatment without additional Mg^{2+} . Data are shown as fold changes compared with 100 CPP2 (set at 100%). Presented data are the mean of three separate experiments consisting of three replicate cultures \pm SD. $P < 0.05$ for CPP2 incubated with *0.8, #2 and \$5 mmol/L Mg^{2+} versus CPP2 concentration-matched formalin-fixed cultures.

Mg^{2+} improves calcification propensity in serum from CKD patients and healthy controls

To examine the effects of Mg^{2+} on serum calcification propensity in CKD patients, the serum of CKD patients and

healthy controls was supplemented with increasing concentrations of Mg^{2+} *ex vivo* and subsequently T_{50} was measured. Serum Mg^{2+} concentration was not different between the groups (0.8 ± 0.2 versus 0.9 ± 0.5 mmol/L). There was a non-significant trend towards a lower baseline T_{50} in CKD patients compared with controls (372 ± 50 versus 323 ± 57 min). The addition of 0.2 mmol/L Mg^{2+} significantly improved T_{50} in donor patients by 51 ± 16 min and CKD patients by 44 ± 13 min (Figure 5A; $P < 0.05$). Each increment of 0.2 mmol/L addition of Mg^{2+} led to a similar increase of ~ 40 min in CKD patients and 50 min in healthy controls (Figure 5B).

DISCUSSION

In this study we demonstrate that Mg^{2+} prevents high Pi-induced VSMC calcification. The preventive effect of Mg^{2+} is mediated via delayed CPP2 formation, because Mg^{2+} is unable to prevent calcification once CPP2 has formed. Specifically, we show that Mg^{2+} does not prevent CPP1 formation. Rather, Mg^{2+} prevents the transition from CPP1 to CPP2. In the sera of CKD patients and healthy controls, a small increase in Mg^{2+} of 0.2 mmol/L improved T_{50} , reflecting a decreased calcification propensity. In addition, our results indicate that crystalline maturation of Pi towards CPP2 is an essential step in VSMC calcification.

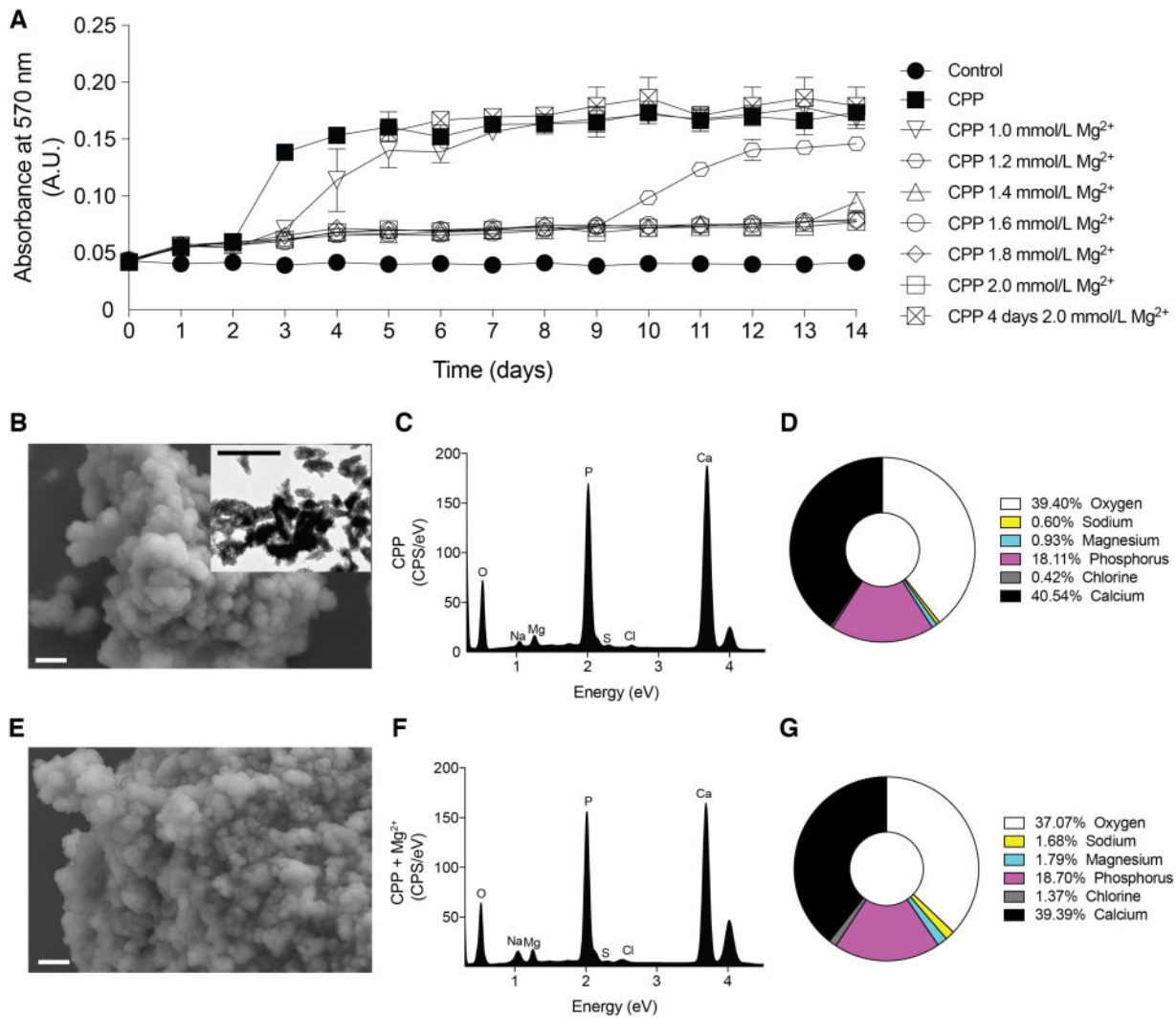


FIGURE 4: Mg²⁺ dose-dependently inhibits the transition from CPP1 to CPP2 and does not affect CPP2 morphology after nucleation. (A) Absorbance of the CPP mixture containing different Mg²⁺ concentrations was measured at 570 nm as a readout for CPP1 (~0.05 AU) to CPP2 (~0.15 AU) transition. This graph is representative of five independently executed experiments each consisting of three replicates. Data are expressed as mean ± SD. A final concentration of 2.0 mmol/L Mg²⁺ after CPP2 (E–G) formation did not alter morphology (SEM) or composition (EDX) compared with control CPP2 (B–D). A TEM picture was inserted in B to confirm CPP2. Scale bars correspond to 300 nm (white) and 500 nm (black).

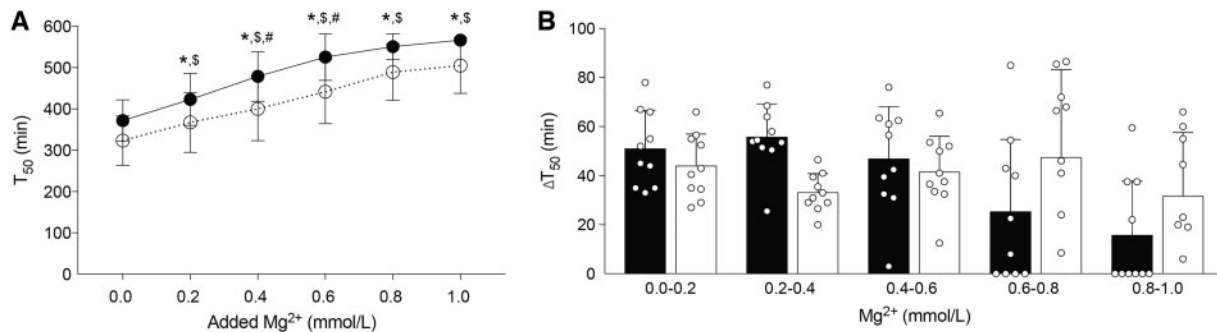


FIGURE 5: Mg²⁺ dose-dependently increases T₅₀ in CKD patient serum. Serum T₅₀ is increased upon Mg²⁺ supplementation of serum from both healthy controls (solid line) and CKD patients (dotted line, A). (B) Change in T₅₀ similar in CKD patients after each addition of Mg²⁺ compared with healthy controls. Black and white bars represent healthy controls and CKD patients, respectively. Data are shown as the mean of 10 patients in each group and are expressed as mean ± SD. P < 0.05 *for healthy controls versus baseline; \$for CKD patients versus baseline and #for CKD patients versus healthy controls at specific Mg²⁺ concentration.

The mechanism by which Mg^{2+} prevents high Pi-induced calcification in CKD models is incompletely understood. Using different *in vitro* models, we demonstrate that Mg^{2+} only prevents Pi-induced VSMC calcification prior to formation of CPP2. After CPP2 formation, Mg^{2+} supplementation did not alter crystal composition and morphology and did not prevent calcification of VSMCs. In addition, Mg^{2+} supplementation did not modify CPP2-induced expression profiles of osteogenic or VSMC contractility genes and proteins. In contrast, Mg^{2+} potently prevents Pi-induced calcification through indirect pathways, as an increased concentration of Mg^{2+} was insufficient to prevent VSMC calcification induced by CPP2. We have shown previously in a bovine model of VSMC calcification that Mg^{2+} blocks Ca^{2+} -Pi crystal formation preceding Pi-induced calcification and independent of transcriptional changes in bovine VSMCs [19]. Other studies have identified the potent anti-crystallization properties of Mg^{2+} [20, 22, 29]. In aqueous solutions, Mg^{2+} is known to stabilize amorphous Ca^{2+} -Pi particles and delay crystal nucleation [30]. Contrarily, another study suggested that the preventive action of Mg^{2+} on VSMC calcification did not depend on the inhibition of CPP2 maturation [31]. For instance, in the study by Louvet *et al.* [31], hydroxyapatite crystals were generated in the presence of hVSMC with 1% FBS only, whereas we used 5% FBS [31]. In low serum conditions, the availability of calcification inhibitors such as fetuin-A is lower, resulting in a milieu that is more prone to calcification. Thus the inhibitory effects of Mg^{2+} on CPP2 formation may potentially be overruled as Pi can precipitate more readily [24].

In our study, Mg^{2+} blocked calcification induced by high Pi, which is consistent with previous studies [15, 16, 18, 32]. When comparing our results, it is important to note that the reported experimental setups have used high Pi to induce VSMC calcification and have supplemented Mg^{2+} immediately in order to prevent calcification [15, 16, 18, 32]. Under these circumstances, it is possible that Mg^{2+} blocked crystal or CPP2 maturation that would otherwise have occurred naturally. Therefore inhibition of Pi-induced calcification may have been secondary to the prevention of CPP2 formation. With high Pi, medium crystals form spontaneously over time. The cellular effects of CPP2-induced calcification are already present 24 h after induction, while those of high Pi-induced calcification only occur after ~1 week. Accordingly, it was shown that crystalline Pi-containing particles induce calcification and VSMC transdifferentiation rather than soluble Pi or amorphous Ca^{2+} -Pi particles (or CPP1) [6, 8, 11].

Calcification propensity (T_{50}) is a risk factor and indicator for cardiovascular morbidity and mortality in CKD patients [23, 33, 34]. To translate the effects of Mg^{2+} on CPP2 maturation to a more clinical setting, we investigated the effects of stepwise Mg^{2+} additions to serum from renal disease patients and healthy controls on T_{50} . Our results demonstrate that Mg^{2+} increased T_{50} by ~50 min per 0.2 mmol/L Mg^{2+} increase in serum from CKD patients and healthy controls. Interestingly, the dose-dependent effects of Mg^{2+} on calcification propensity are similar in both groups. These *ex vivo* results are consistent with a previous study in patients on dialysis [35, 36]. It was demonstrated that Mg^{2+} effectively and promptly increased T_{50}

by 72 min once dialysate Mg^{2+} was adjusted from 0.5 to 1.0 mmol/L, which resulted in a serum increase of 0.36 mmol/L [36]. Dialysate Mg^{2+} supplementation increased T_{50} without modifying intracellular Mg^{2+} concentrations, consistent with the notion that serum Mg^{2+} is key to modify calcification propensity [36]. The ability of Mg^{2+} to potently modify T_{50} is of great clinical interest. Given the sensitivity of T_{50} for Mg^{2+} , this relationship should be clinically exploited. Further clinical studies should investigate whether *ex vivo* determinations of calcification propensity could be used to define optimal dialysate or oral Mg^{2+} concentration for CKD patients.

Our results indicate that cellular Pi toxicity leading to calcification is determined by the presence of crystalline Pi in the form of CPP2. Efforts to prevent vascular calcification are currently aimed at lowering serum Pi concentrations in CKD patients. Importantly, management of serum Pi by Pi binders is insufficient to decrease the risk for cardiovascular disease and vascular calcification in CKD [37]. Instead, determinants affecting the transition from Pi towards crystalline Pi (CPP2) potentially prove to be more clinically relevant. Mg^{2+} prevented VSMC calcification *in vitro* despite high Pi concentrations and improved calcification propensity in humans without normalizing serum Pi concentrations [19, 36]. In addition, increased serum Mg^{2+} (>1.27 mmol/L) neutralizes the association between serum Pi concentration and the risk for cardiovascular mortality [38]. Therefore Mg^{2+} potentially disarms Pi toxicity in CKD without changing the soluble Pi concentration itself. As such, Pi toxicity, and therefore calcification risk, should be clinically determined based on Pi crystallinity.

This is the first study that uses CPP2-induced VSMC calcification to distinguish intracellular effects from extracellular effects of Mg^{2+} . In addition, our approach includes *in vitro* models and an *ex vivo* study coupling the effects of Mg^{2+} to calcification propensity. Although we demonstrate that Mg^{2+} limits VSMC calcification primarily through the inhibition of CPP2 maturation already at small incremental concentrations, we cannot exclude potential contributing effects of intracellular pathways related to calcification. While the results presented here need to be verified *in vivo*, our conclusions may have important implications for clinical interpretation of the effects of Mg^{2+} on calcification. Recently a longer-term randomized clinical study using oral magnesium oxide supplements showed halted progression of coronary artery calcification in pre-dialysis CKD patients [39]. Another study is currently being initiated (ClinicalTrials.gov identifier NCT02542319) [40]. These studies are a major step towards improving cardiovascular outcomes in CKD patients using Mg^{2+} supplements.

In conclusion, our study demonstrates that Mg^{2+} prevents hVSMC calcification by inhibition of CPP2 maturation *in vitro*. In serum from CKD patients, Mg^{2+} increased T_{50} in a dose-dependent manner. Increasing serum Mg^{2+} may be a promising treatment to target pathological CPP2 maturation in CKD-induced vascular calcification.

SUPPLEMENTARY DATA

Supplementary data are available at [ndt](http://ndt.oxfordjournals.org/) online.

ACKNOWLEDGEMENTS

The authors thank Huib Croes and Caro Bos (both from the Radboud University Medical Center, Nijmegen, The Netherlands) and Dr Swapna Karthik (Calcison, Bern, Switzerland) for their wonderful technical assistance. The authors also thank Dr Jan-Luuk Hillebrands (University Medical Center Groningen, Groningen, The Netherlands) for sharing his expertise related to calciprotein particle synthesis.

FUNDING

This research was funded by grants from the Netherlands Organization for Scientific Research (NWO Veni 016.186.012 and VICI 016.130.668) and the Dutch Kidney Foundation (Kolff 14OKG17 and 15OP02). This work was furthermore supported by the NIGRAM2+ consortium, funded by Health Holland (LSHM17034) and the Dutch Kidney Foundation (16TKI02).

AUTHORS' CONTRIBUTIONS

A.D.t.B., J.H.F.d.B., C.E., J.G.J.H. and M.H.d.B. were involved in the conception and design of the experiments. A.D.t.B., C.E., A.P. and L.W.Z. performed experiments and analysed data. S.J.L.B. recruited patients and founded the TransplantLines cohort study. A.D.t.B. drafted the manuscript. A.D.t.B., J.H.F.d.B., C.E., J.G.J.H., A.P. and M.H.d.B. critically revised the manuscript. All authors approved the final version of the manuscript.

CONFLICT OF INTEREST STATEMENT

M.H.d.B. has served as a consultant or received honoraria (to employer) from Amgen, Bayer, Kyowa Kirin Pharma, Sanofi Genzyme and Vifor Fresenius Medical Care Renal Pharma. A.P. is the inventor of the T₅₀ test and co-founder, shareholder and employee of Calcison.

REFERENCES

1. Sigrist MK, Taal MW, Bungay P *et al.* Progressive vascular calcification over 2 years is associated with arterial stiffening and increased mortality in patients with stages 4 and 5 chronic kidney disease. *Clin J Am Soc Nephrol* 2007; 2: 1241–1248
2. Ishimura E, Okuno S, Yamakawa T *et al.* Serum magnesium concentration is a significant predictor of mortality in maintenance hemodialysis patients. *Magn Res* 2007; 20: 237–244
3. Sakaguchi Y, Fujii N, Shoji T *et al.* Hypomagnesemia is a significant predictor of cardiovascular and non-cardiovascular mortality in patients undergoing hemodialysis. *Kidney Int* 2014; 85: 174–181
4. Salem S, Bruck H, Bahlmann FH. Relationship between magnesium and clinical biomarkers on inhibition of vascular calcification. *Am J Nephrol* 2012; 35: 31–39
5. Floege J. Magnesium concentration in dialysate: is higher better? *Clin J Am Soc Nephrol* 2018; 13: 1309–1310
6. Aghagolzadeh P, Bachtler M, Bijarnia R *et al.* Calcification of vascular smooth muscle cells is induced by secondary calciprotein particles and enhanced by tumor necrosis factor- α . *Atherosclerosis* 2016; 251: 404–411
7. Viegas CSB, Santos L, Macedo AL *et al.* Chronic kidney disease circulating calciprotein particles and extracellular vesicles promote vascular calcification. *Arterioscler Thromb Vasc Biol* 2018; 38:575–587
8. Sage AP, Lu J, Tintut Y *et al.* Hyperphosphatemia-induced nanocrystals upregulate the expression of bone morphogenetic protein-2 and osteopontin genes in mouse smooth muscle cells in vitro. *Kidney Int* 2011; 79: 414–422
9. Moe SM, Chen NX. Mechanisms of vascular calcification in chronic kidney disease. *J Am Soc Nephrol* 2008; 19: 213–216
10. Kapustin AN, Chatrou MLL, Drozdov I *et al.* Vascular smooth muscle cell calcification is mediated by regulated exosome secretion. *Circ Res* 2015; 116: 1312–1323
11. Proudfoot D, Shanahan CM. Nanocrystals seed calcification in more ways than one. *Kidney Int* 2011; 79: 379–382
12. Shanahan CM, Crouthamel MH, Kapustin A *et al.* Arterial calcification in chronic kidney disease: key roles for calcium and phosphate. *Circ Res* 2011; 109: 697–711
13. Massy ZA, Drüeke TB. Magnesium and cardiovascular complications of chronic kidney disease. *Nat Rev Nephrol* 2015; 11: 432–441
14. Herencia C, Rodriguez-Ortiz ME, Munoz-Castaneda JR *et al.* Angiotensin II prevents calcification in vascular smooth muscle cells by enhancing magnesium influx. *Eur J Clin Invest* 2015; 45: 1129–1144
15. Montezano AC, Zimmerman D, Yusuf H *et al.* Vascular smooth muscle cell differentiation to an osteogenic phenotype involves TRPM7 modulation by magnesium. *Hypertension* 2010; 56: 453–462
16. Kircelli F, Peter ME, Sevinc Ok E *et al.* Magnesium reduces calcification in bovine vascular smooth muscle cells in a dose-dependent manner. *Nephrol Dial Transplant* 2012; 27: 514–521
17. Louvet L, Metzinger L, Büchel J *et al.* Magnesium attenuates phosphate-induced deregulation of a microRNA signature and prevents modulation of Smad1 and Osterix during the course of vascular calcification. *Biomed Res Int* 2016; 2016: 1–11
18. De Oca AM, Guerrero F, Martinez-Moreno JM *et al.* Magnesium inhibits wnt/b-catenin activity and reverses the osteogenic transformation of vascular smooth muscle cells. *PLoS One* 2014; 9: 1–10
19. ter Braake AD, Tinnemans PT, Shanahan CM *et al.* Magnesium prevents vascular calcification in vitro by inhibition of hydroxyapatite crystal formation. *Sci Rep* 2018; 8: 2069
20. Blumenthal NC, Betts F, Posner AS. Stabilization of amorphous calcium phosphate by Mg and ATP. *Calcif Tissue Res* 1977; 23: 245–250
21. Boistelle R, Lopez-Valero I, Abbona F. Cristallisation des phosphates de calcium en présence de magnésium. *Nephrologie* 1993; 14: 265–269
22. Boskey AL, Posner AS. Magnesium stabilization of amorphous calcium phosphate: a kinetic study. *Mater Res Bull* 1974; 9: 907–916
23. Keyzer CA, de Borst MH, van den Berg E. Calcification propensity and survival among renal transplant recipients. *J Am Soc Nephrol* 2015; 27: 1–10
24. Pasch A, Farese S, Graber S *et al.* Nanoparticle-based test measures overall propensity for calcification in serum. *J Am Soc Nephrol* 2012; 23: 1744–1752
25. Smith ER, Cai MM, McMahon LP *et al.* Serum fetuin-A concentration and fetuin-A-containing calciprotein particles in patients with chronic inflammatory disease and renal failure. *Nephrology (Carlton)* 2013; 18: 215–221
26. Smith ER, Ford ML, Tomlinson LA *et al.* Phosphorylated fetuin-A-containing calciprotein particles are associated with aortic stiffness and a procalcific milieu in patients with pre-dialysis CKD. *Nephrol Dial Transplant* 2012; 27: 1957–1966
27. Smith ER, Hewitson TD, Hanssen E *et al.* Biochemical transformation of calciprotein particles in uraemia. *Bone* 2018; 110: 355–367
28. Eisenga MF, Gomes-Neto AW, Van Londen M *et al.* Rationale and design of TransplantLines: a prospective cohort study and biobank of solid organ transplant recipients. *BMJ Open* 2018; 8: e024502
29. Apfelbaum F, Mayer I, Rey C *et al.* Magnesium in maturing synthetic apatite: a Fourier transform infrared analysis. *J Cryst Growth* 1994; 144: 304–310
30. Abbona F, Baronnet A. A XRD and TEM study on the transformation of amorphous calcium phosphate in the presence of magnesium. *J Cryst Growth* 1996; 165: 98–105
31. Louvet L, Bazin D, Büchel J *et al.* Characterisation of calcium phosphate crystals on calcified human aortic vascular smooth muscle cells and potential role of magnesium. *PLoS One* 2015; 10: e0115342
32. Louvet L, Büchel J, Steppan S *et al.* Magnesium prevents phosphate-induced calcification in human aortic vascular smooth muscle cells. *Nephrol Dial Transplant* 2013; 28: 869–878